
Figures and figure supplements

Associative plasticity of granule cell inputs to cerebellar Purkinje cells

Rossella Conti and Céline Auger.

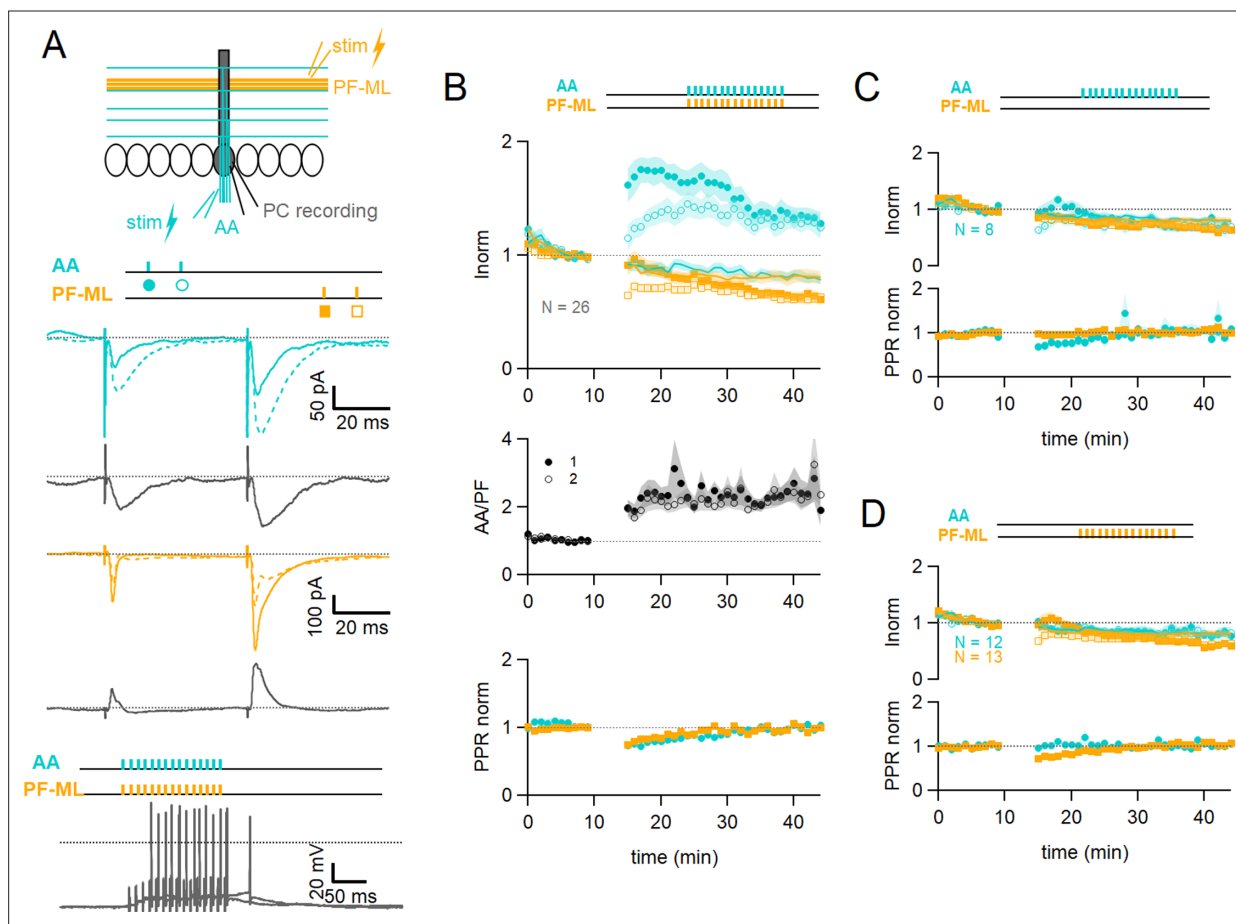


Figure 1. Associative plasticity of ascending axon (AA) and parallel fibre (PF) inputs. **(A, top)** Whole-cell recording in a Purkinje cell (PC). Two stimulation electrodes are used to activate granule cell (GC) inputs: one in the molecular layer to stimulate PFs (orange), and one in the GC layer to stimulate AAs (blue). The test stimulation protocol is depicted with colours and symbols as used in the plots in the following sections for the first (closed) and the second excitatory postsynaptic currents (EPSCs) (open). **(Middle)** AA- and PF-PSCs were sampled with a pair of pulses (dt=50 ms), every 10 s. Traces from one experiment: average AA-PSC (blue) and PF-PSC (orange), before (5–10 min, continuous line) and after the induction protocol (25–30 min, dotted line). Subtraction in grey. AA-EPSC amplitude increased while PF-EPSC amplitude decreased. No antagonist was applied. Evoked responses consisted of an EPSC often followed by an IPSC. **(Bottom)** induction protocol. Recording switched to current clamp, $V_H = -65$ mV. AAs and PFs are stimulated synchronously by a train of 15 pulses at 100 Hz every 3 s for 5 min. Grey traces, responses to the first two trains of stimulation. **(B Top)** a plot of the average AA- and PF-EPSC amplitude normalised to baseline for synchronous stimulation (5–10 min, $n=26$, colours and symbols as in A) and control No Stim experiments (continuous lines). Following induction, a long-term change in the inputs was observed. The amplitude of the AA-EPSC increased to $131 \pm 7\%$ ($n=24$) of baseline 25–30 min after induction ($p=7e-5$ one-tailed T-test, $n=24$). The PF-EPSC on the other hand decreased slowly to $65 \pm 5\%$ ($n=25$) of baseline ($p=1e-7$ one-tailed T-test, $n=25$). Continuous lines show the average time course of AA- and PF-EPSC amplitudes during control No Stim experiments where no stimulation was performed during the clamp period ($n=17$, see **Figure 1—figure supplement 1**), showing the extent of EPSC rundown during the course of the recordings. **(Middle)** the average ratio of the normalised amplitudes of AA- and PF-EPSCs (AA/PF), highlighting the relative change of the inputs, doubles. **(Bottom)** the average normalised paired-pulse ratio (AA2/AA1 and PF2/PF1) is transiently decreased following induction. **(C)** Average of eight experiments with stimulation of the AA pathway only during induction (labels, colours, and symbols as in A), and No Stim experiments overlaid (continuous lines). **(Top)** the normalised amplitudes of AA- and PF-EPSCs progressively decreased to $72 \pm 7\%$ ($n=8$) and $64 \pm 6\%$ ($n=8$) of baseline respectively, not significantly different from No Stim experiments ($p=0.49$ and $p=0.48$, respectively). Stimulation of the AA pathway alone is not sufficient to trigger AA-LTP. **(D)** Average of 13 experiments with stimulation of the PF pathway only during induction (labels), and No Stim experiments overlaid (continuous lines). **(Top)** the normalised AA-EPSCs showed a small and steady depression ($84 \pm 7\%$ of baseline after 25–30 min) whereas the PF-EPSC depressed over time ($64 \pm 6\%$), not significantly different from No Stim experiments ($p=0.63$ and $p=0.25$, respectively). Stimulation of the PF pathway on its own is not sufficient to trigger plasticity. **(C and D bottom)** the PPR of the AA and PF pathways transiently decreased only for the pathway stimulated during induction. Values given are mean \pm SEM. SEM is represented by shading. Statistical significance was tested using the Wilcoxon Mann Whitney test except for control data tested using T-test.

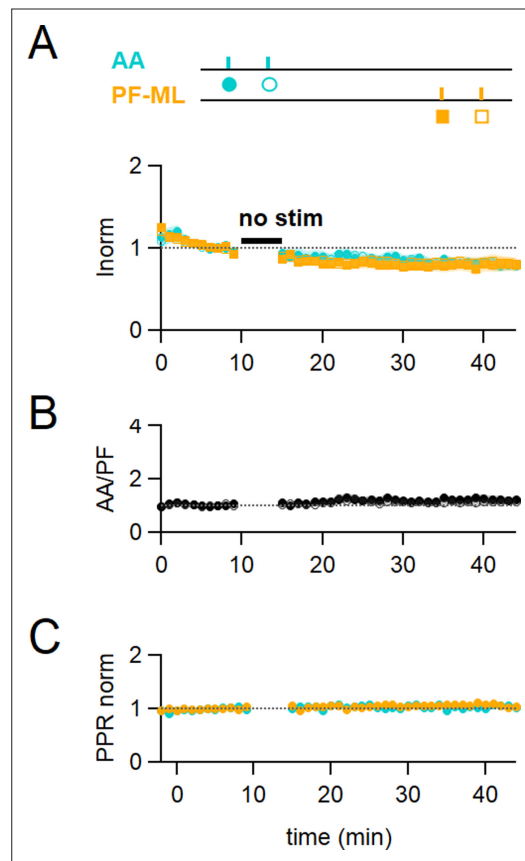


Figure 1—figure supplement 1. Control No Stim experiments. **(A)** Plot of the average ascending axon (AA)- and parallel fibre (PF)-excitatory postsynaptic current (EPSC) amplitude normalised to baseline ($n=17$, colours and symbols shown on the experimental protocol). No stimulation was applied during the 5 min IClamp period. Rundown of the AA- and PF-EPSCs peak amplitude was observed throughout the experiments. On average, the amplitude of the AA-EPSC and PF-EPSC decreased to $80 \pm 6\%$ ($n=16$, significantly smaller than baseline $P=0.0004$) and $81 \pm 8\%$ ($n=17$, not significantly smaller than baseline $p=0.062$) of baseline 25–30 min after induction, respectively, indicating a rundown of the amplitude for both pathways during experimental time, independent of the induction protocol. **(B)** The average ratio of the normalised amplitudes of AA- and PF-EPSCs showing relative stability of the inputs following the No Stim protocol. **(C)** The average normalised paired pulse ratio (AA2/AA1 and PF2/PF1) is unchanged. Values given are mean \pm SEM. SEM is represented by shading. Statistical significance was tested using the Wilcoxon Mann Whitney test.

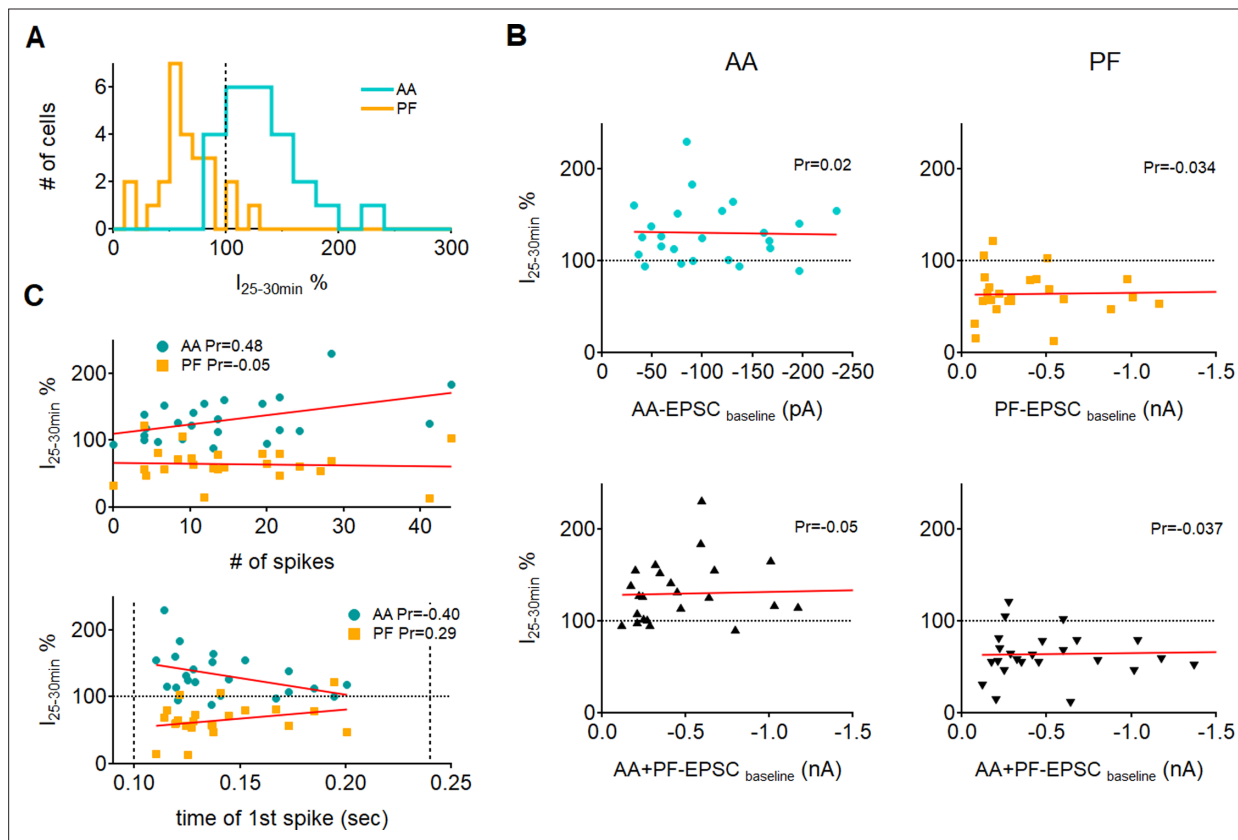


Figure 1—figure supplement 2. Effect of excitatory postsynaptic current (EPSC) amplitude and spiking of the Purkinje cell on plasticity. **(A)** Histogram showing the distribution of long-term changes of ascending axon (AA)- and parallel fibre (PF)-EPSCs for all control cells. Data is normally distributed. **(B, Top)** plots of long-term changes of AA- and PF-EPSCs amplitudes for control cells as a function of the baseline EPSC amplitude ($n=24$ for AA and $n=25$ for PF). The red line represents the linear fit of the data. No correlation was observed between plastic changes and the initial amplitude of the response, as indicated by the Pearson's coefficients of linear regression (Pr). **Bottom:** long-term changes plotted as a function of the sum of baseline AA and PF amplitudes to check for a cooperative effect of the inputs. Again, no correlation was found between the long-term plasticity outcome and the total amplitude of synaptic currents, as indicated by the linear fits and regression coefficients. **(C)** Plots of long-term changes in AA and PF amplitudes as a function of the number of spikes evoked by synchronous stimulation during induction (**top**) and the time at which the first spike was fired (**bottom**, dotted vertical bars indicate the beginning and end of the stimulus train). For each cell, the number of spikes and the time of the first spike are averaged over the first 5 trains of stimulation. The decrease in PF responses was independent of the number of spikes evoked or the time at which the first spike was fired (Pr: Pearson's coefficient of linear regression). For AA responses instead, there was a moderate positive correlation between the level of long-term potentiation (LTP) and the number of spikes, and a moderate negative correlation between the level of LTP and the time at which the first spike was fired, indicating a weak dependence of AA plasticity on spiking during induction.

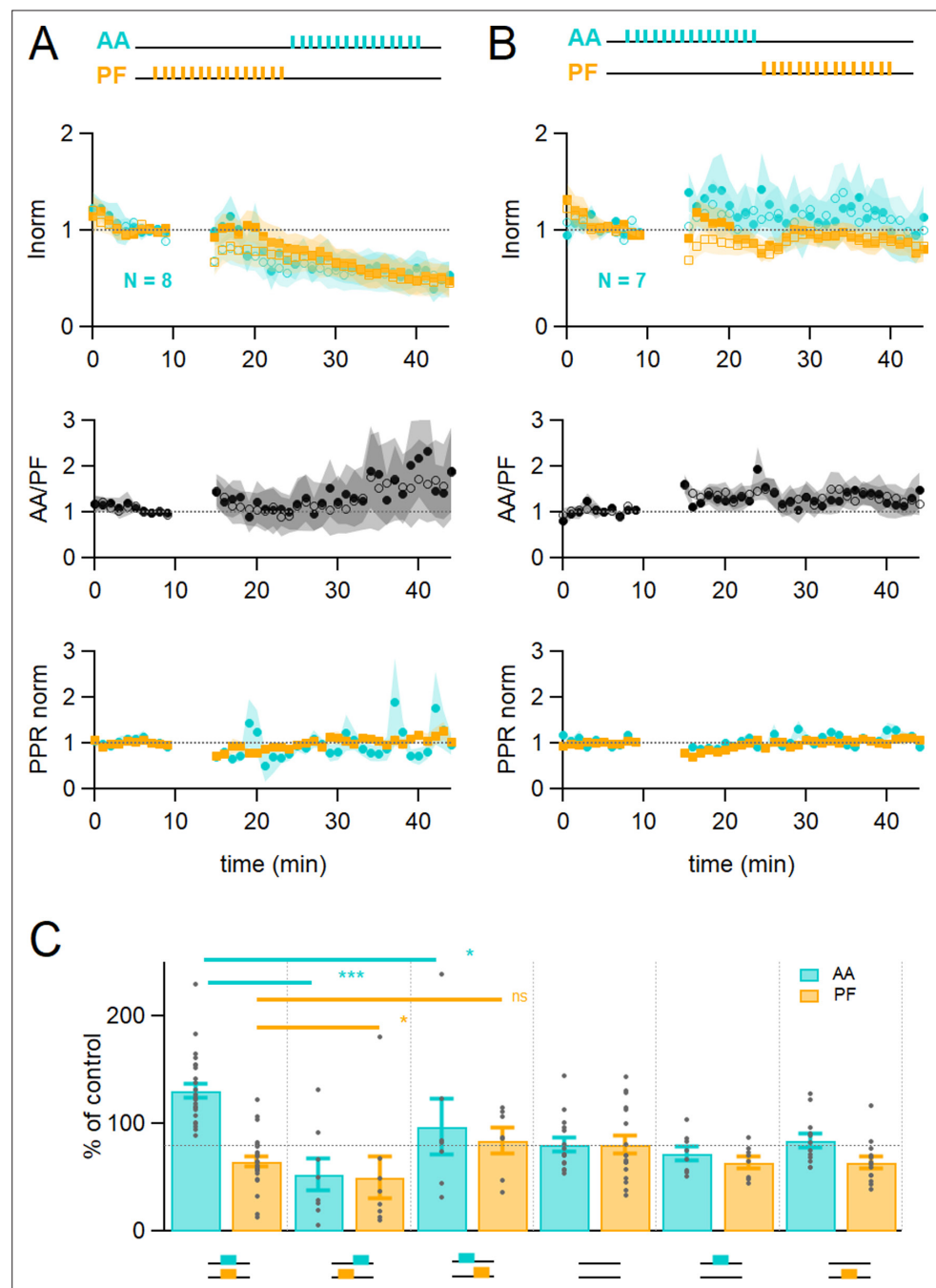


Figure 2. Time dependence of plasticity. (A) On average, when stimulating ascending axons (AAs) 150 ms after parallel fibres (PFs), the AA- and PF-excitatory postsynaptic currents (EPSCs) decreased by a similar extent (AA was $53 \pm 15\%$, PF $50 \pm 20\%$ of control, $n=8$, not significantly different from each other $p=0.84$). These changes were significantly different from experiments with synchronous stimulation ($p=8e-5$ for AA and $p=0.022$ for PF). The relative normalised amplitude of the AA pathway increased but not significantly (AA/PF was $224 \pm 75\%$ of control, $n=7$, $p=0.2$). Colour coding for AA and PF input pathways. Closed symbols for the first and open symbols for the second EPSCs. (B) When stimulating AAs 150 ms before PFs, the AA-EPSC facilitated, but declined back to baseline (AA was $97 \pm 26\%$ of control, $n=7$, significantly smaller than synchronous stimulation $p=0.011$), and the PF-EPSC was maintained close to baseline (PF $84 \pm 12\%$ of control, $n=7$, not significantly larger than synchronous stimulation, $p=0.062$). The relative normalised amplitude of the AA pathway and the PPR were not affected significantly (AA/PF was $126 \pm 31\%$ of control, $p=0.35$, and $PPR_{AA} = 114.4 \pm 6.4\%$, $PPR_{PF} = 107.1 \pm 4.6\%$, $n=7$). (C) Average amplitude at 25–30 min as a percentage of baseline for various timing of stimulation, control No Stim, AA only, and PF only stimulation. Individual data points are overlaid for each type of experiment. The AA-EPSC was

Figure 2 continued on next page

Figure 2 continued

131 ± 7% of baseline (n=24) 25–30 min after induction when AA and PF stimulation was synchronous. It was 53 ± 15% (n=8) when AA stimulation was delayed by 150 ms, and 97 ± 26% (n=7) when PF stimulation was delayed by 150 ms. The PF-EPSC was 65 ± 5% of baseline (n=25) when stimulation was synchronous, 50 ± 20% (n=8) when AA stimulation was delayed by 150 ms, and 84 ± 12% (n=7) when PF stimulation was delayed by 150 ms. The horizontal dotted line indicates EPSC amplitude at the end of the No Stim experiments. (**p<0.001, *p<0.05, ns: not significant). Values given are mean ± SEM. SEM is represented by shading. Wilcoxon Mann Whitney tests.

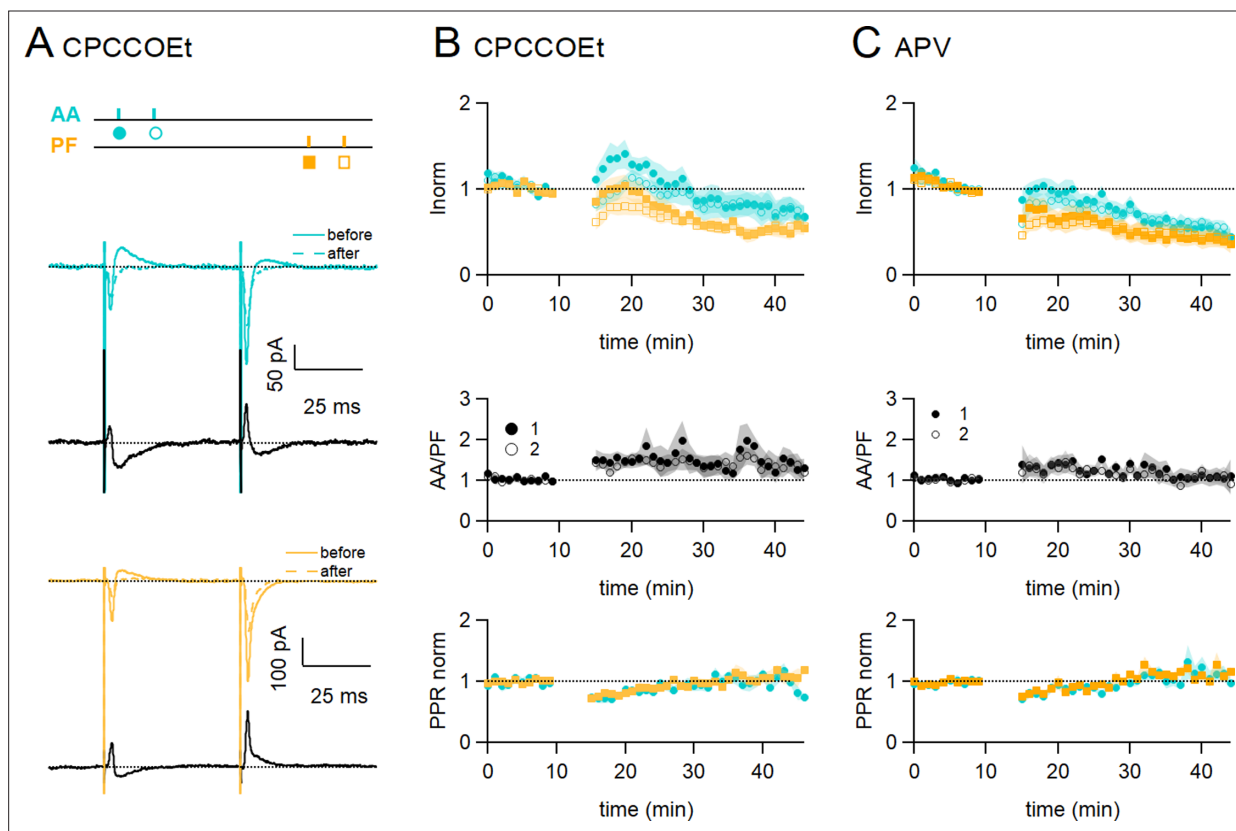


Figure 3. Role of NMDARs and mGluR1s. **(A)** Bath application of CPCCOEt (50 μ M), a selective blocker of mGluR1Rs, strongly inhibits long-term potentiation (LTP) of ascending axon (AA)-excitatory postsynaptic currents (EPSCs). Sample recordings from one experiment. Traces are the average of the AA (blue) and parallel fibre (PF) (orange) synaptic responses, before (5–10 min, continuous line) and after induction (25–30 min, dotted line). Subtraction traces (25–30 min - 5–10 min) in black. A decrease in the AA-EPSC and PF-EPSC is observed. The test stimulation protocol is depicted with colours and symbols as used in the plots in the following sections for the first (closed) and the second EPSCs (open). **(B, Top)** Average time course of the normalised AA- and PF-EPSCs (n=8). mGluR1 receptor block impairs AA-LTP. AA was $72 \pm 13\%$ of baseline (statistically smaller than control synchronous stimulation $p=0.0004$, $n=7$ and $n=24$, and the PF-EPSC was $54 \pm 8\%$, $n=7$, not significantly smaller than control synchronous stimulation, $p=0.12$, $n=7$) **(Middle)** a small sustained increase in the ratio of normalised amplitudes (AA/PF) is observed. **(Bottom)** Plot of the normalised PPR of both inputs. **(C, Top)** Average time course of the normalised AA- and PF-EPSCs (colours and symbols as in A) in the presence of APV (50 μ M) (n=7). Both AA and PF pathways are depressed, showing that NMDAR activation is necessary for AA-LTP induction. The AA- and PF-EPSCs were on average $50 \pm 8\%$ and $40 \pm 9\%$ of baseline 25–30 min after induction (n=6, significantly smaller than control $p=2e-6$, and $n=7$, $p=0.027$, respectively) **(Middle)** The ratio of normalised amplitudes (AA/PF) is slightly increased, reflecting a slower depression of the AA inputs. **(Bottom)** Plot of the normalised PPR of both inputs. Values given are mean \pm SEM. SEM is represented by shading. Wilcoxon Mann Whitney tests.

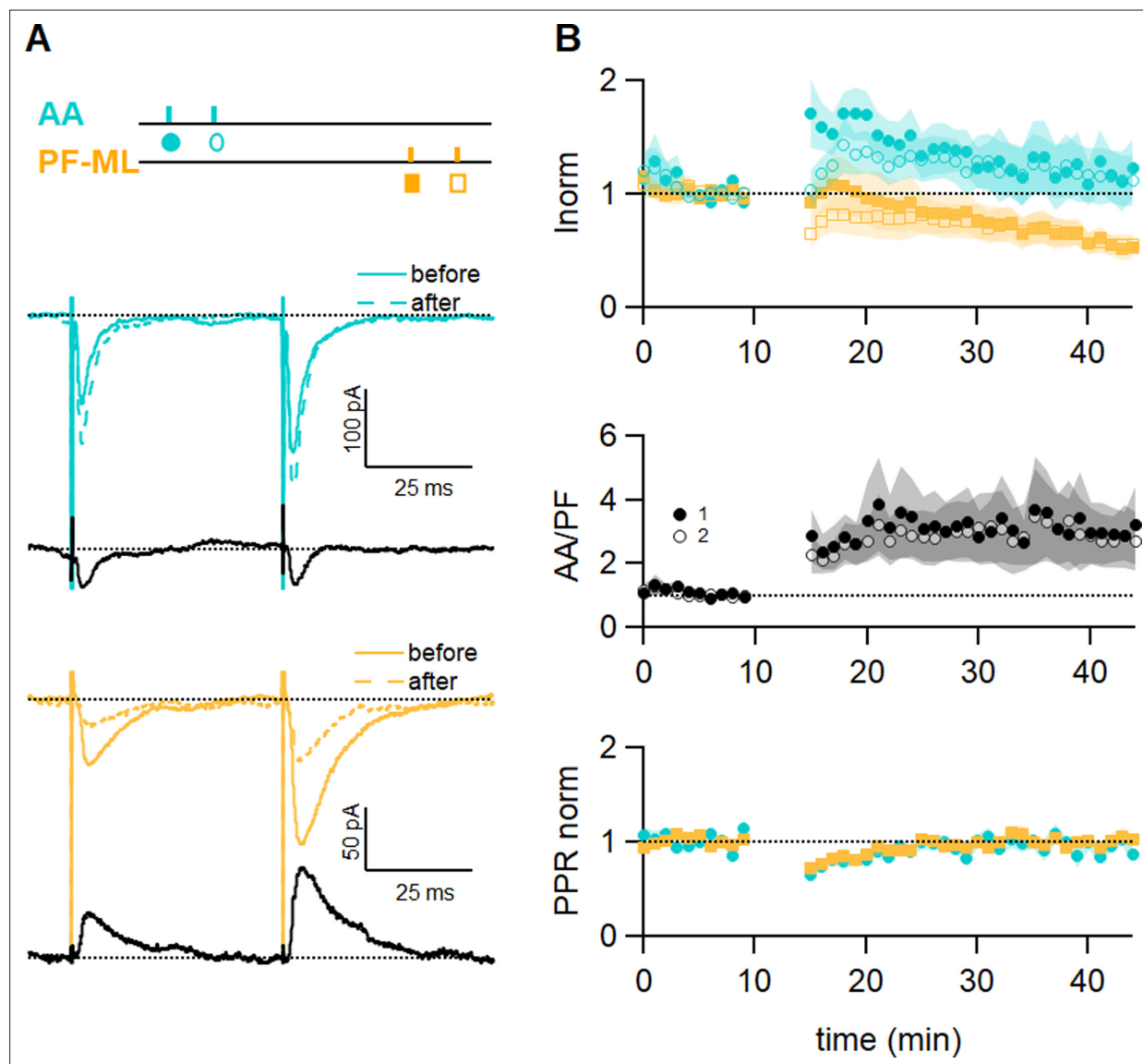


Figure 4. GABA_A receptor block affects long-term plastic changes. **(A)** Sample recordings from an experiment in the presence of the GABA_AR antagonist SR (3 μ M). Paired excitatory postsynaptic currents (EPSCs) evoked before and after induction, together with subtraction traces (black), are shown for the ascending axon (AA) (blue) and parallel fibre (PF) (orange) pathways. The AA-EPSC is increased after induction and the PF-EPSC is strongly decreased in this experiment. The test stimulation protocol is depicted with colours and symbols as used in the plots in the following section for the first (closed) and the second EPSCs (open). **(B)** Average time course of the normalised AA- and PF-EPSCs ($n=9$). The big errors in AA peak amplitude observed after induction are due to the large variability of the outcome of the protocol on this pathway (AA $117 \pm 24\%$; PF $56 \pm 10\%$, $n=9$; not significantly different from control experiments $p=0.1$ and not significantly smaller than control values $p = 0.19$ respectively, Wilcoxon Mann Whitney tests). The ratio of the normalised AA and PF amplitude shows the same variability, while the normalised PPR displays the same relative error and time course as control experiments. Values given are mean \pm SEM. SEM is represented by shading.

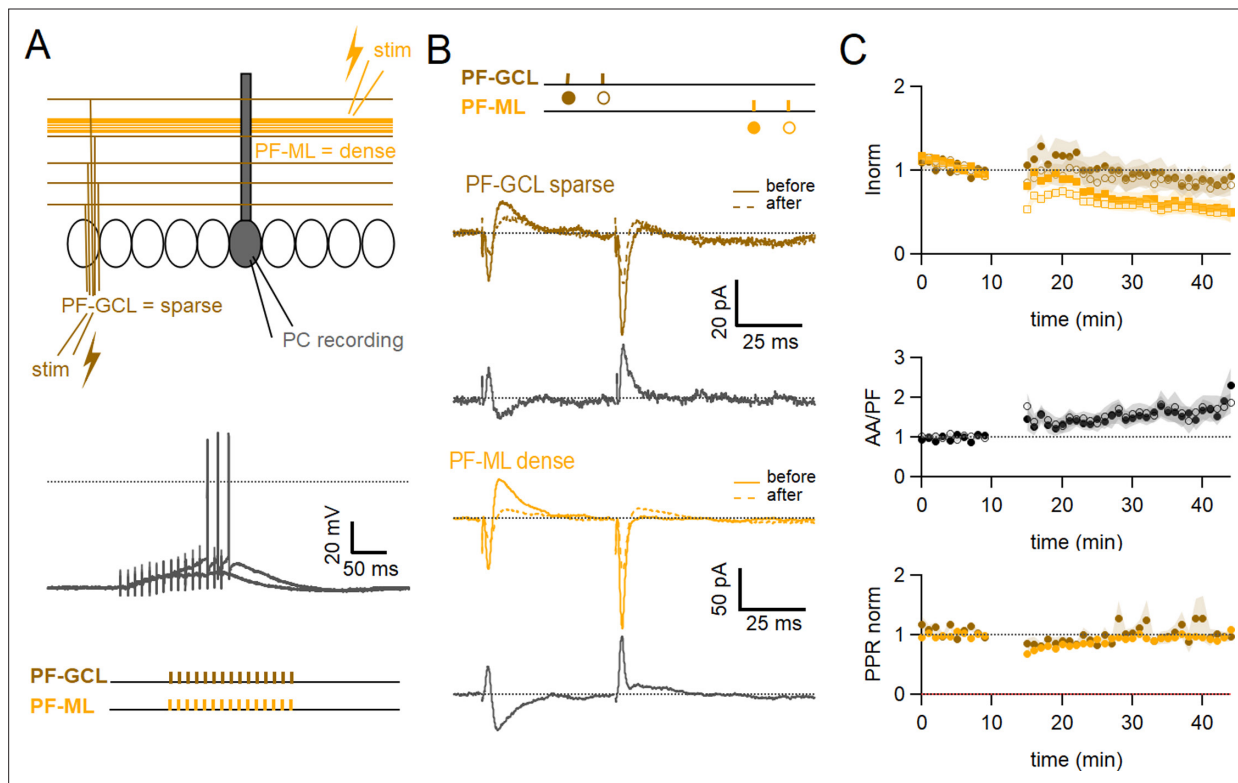


Figure 5. Role of the sparse input distribution. **(A)** To test the role of the sparse input distribution, a stimulation electrode was positioned in the granule cell (GC) layer, stimulating only parallel fibre (PF) synapses sparsely distributed on the PC dendrites. The induction protocol was applied to the sparse PF pathway (PF-sparse), together with the dense PF pathway stimulated in the molecular layer (PF-dense). **(B)** Example experiment. Traces show the PF-sparse and -dense excitatory postsynaptic currents (EPSCs) before and after induction, and subtractions (grey) to highlight changes. The test stimulation protocol is depicted with colours and symbols as used in the plots in the following section for the first (closed) and the second EPSCs (open). 25–30 min after induction, both the sparse and dense EPSCs are reduced. **(Bottom left)** IClamp responses to the first two trains of stimulation. **(C)** Average time course of the normalised EPSC amplitudes ($n=10$). Both sparse and dense inputs are reduced on average to $88\% \pm 13\%$ (significantly smaller than control AA, $p=0.0024$, $n=10$ PF-sparse and $n=24$ AA control) and $54 \pm 10\%$ of baseline (significantly smaller than control PF, $p=0.017$, $n=10$ PF-dense and $n=25$ PF control) after 25–30 min, respectively. With time, the dense PF input was more strongly depressed, and the ratio of normalised amplitudes (PF-sparse/PF-dense) increased to $182\% \pm 24\%$ of control. Values given are mean \pm SEM. SEM is represented by shading. Wilcoxon Mann Whitney tests.

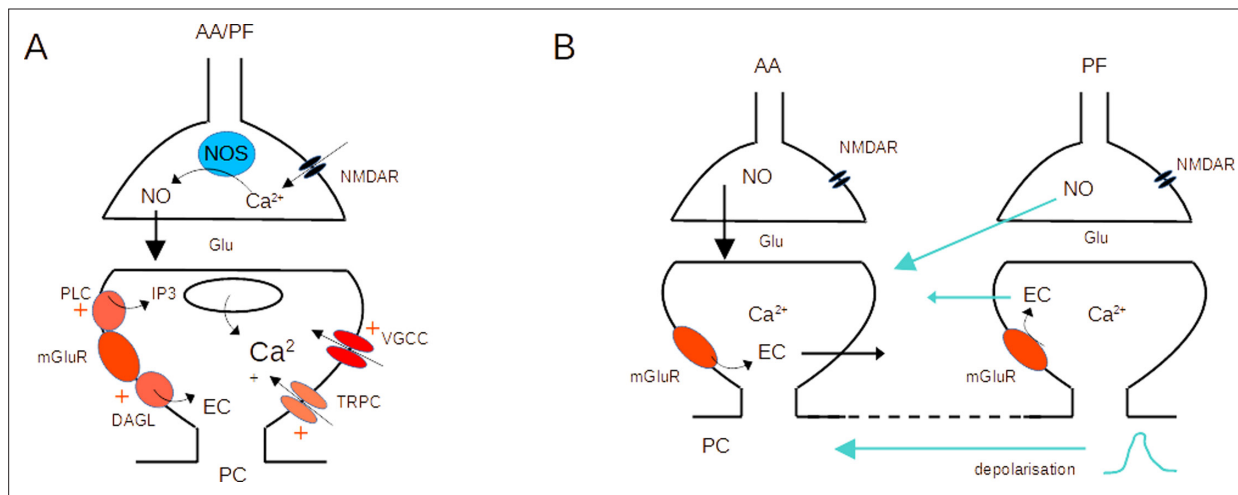
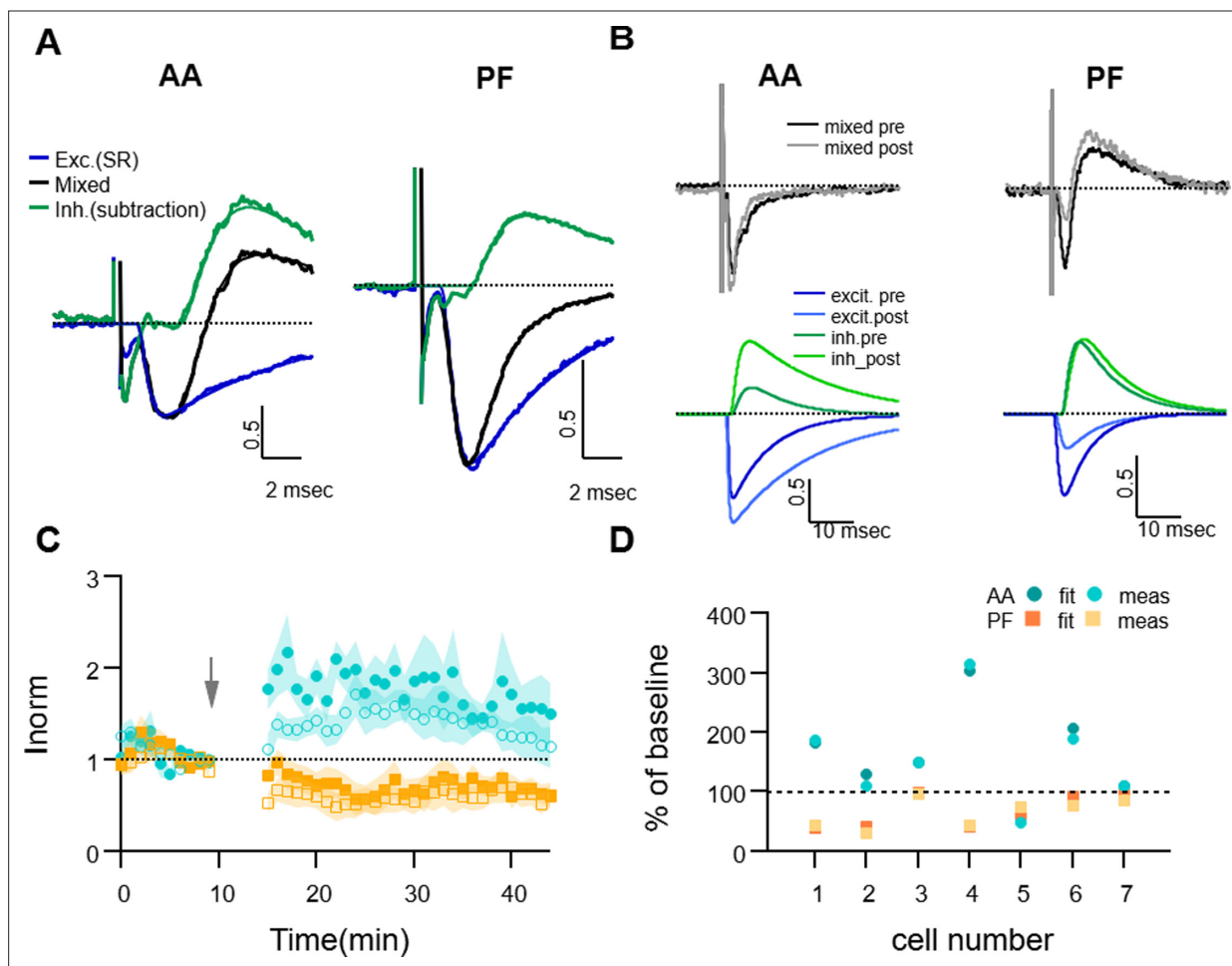


Figure 6. Molecular pathways and potential crosstalk mechanisms involved in AA-long-term potentiation (LTP). **(A)** Activation of presynaptic NMDARs triggers Ca^{2+} entry, activation of NOS, and production of NO. NO diffuses to the postsynaptic compartment where it triggers Guanylate Cyclase activation and regulation of AMPAR number. Activation of postsynaptic mGluR1s in the PC activates PLC, DAGL, TRPC, and a modulation of VGCC, triggering an increase in the Ca^{2+} concentration and EC production. NO and Ca^{2+} concentration control plasticity (Bouvier et al., 2016). **(B)** The dendritic depolarisation triggered by activation of the dense patch of PF synapses might prime Ca^{2+} release from stores linked to mGluR1 activation. Alternatively, NO or EC produced at PF synapses might diffuse to AA synapses. Potential sources of crosstalk are highlighted in blue. AA ascending axon, DAGL Diacylglycerol lipase, EC Endocannabinoids, Glu glutamate, NO Nitric Oxide, NOS Nitric Oxide Synthase, PC Purkinje cell, PF parallel fibre, PLC phospholipase C, TRPC Transient receptor potential canonical channel, VGCC voltage-gated calcium channels.



Appendix 1—figure 1. Dissecting excitation and inhibition shows that excitatory postsynaptic current (EPSC) amplitude and long term changes are well estimated with the direct measure method. **(A)** Fitting procedure used to extract the excitatory and inhibitory components of the recorded mixed PSCs (EPSC + IPSC). Traces recorded during the baseline period were normalised to the peak excitatory response and then averaged over all cells. The mixed evoked PSC (black thick line) is shown together with the excitatory response recorded during SR application (blue thick line). The inhibitory trace (green thick line) is the difference between the mixed PSC and the fit of the excitatory response. The EPSC and inhibitory postsynaptic current (IPSC) fitting functions as well as the mixed fitting function resulting from the sum of the two are overlaid (thinner lines, same colour), showing good agreement with the data. On average, inhibition was delayed and relatively smaller than excitation for both ascending axon (AA) and parallel fibre (PF) pathways. **(B)** Sample traces for an experiment where the excitatory and inhibitory components were extracted from the mixed PSC for both the baseline and 25–30 min after induction; top: mixed PSCs for AA (left) and PF (right) before and after induction; below are the corresponding excitatory (blue, dark and light for pre and post-induction, respectively) and inhibitory components (green, dark and light for pre and post-induction, respectively). The AA-EPSC increased and the PF-EPSC decreased, while both AA- and PF-IPSCs increased in this example. **(C)** Average time course of the EPSCs relative amplitude (measured with the standard minimum amplitude method) for seven experiments in which gabazine (SR) was applied transiently 20 min before and 30 min after long-term potentiation (LTP) induction. Peak EPSCs amplitudes of the first and second evoked responses in the pair for both AA (blue, closed circles: first response in the pair, open circles: second response) and PF (orange, closed squares: first response in the pair, open squares: second response) stimulation. Short and long-term plastic changes are not different from control experiments. **(D)** The normalised EPSC amplitude 25–30 min after induction is compared for the two analysis methods for each cell, either measured directly as the minimum of the recorded response (meas) or that of the excitatory fitting function (fit). Disynaptic inhibition only slightly affected the measure of the real excitatory peak, both for AA- (blue triangles) and PF-EPSC (orange circles) (AA measured: $160 \pm 30\%$, from fit: $160 \pm 30\%$ and PF measured: $65 \pm 9\%$, from fit: $70 \pm 10\%$).